Ab Initio and Electron Propagator Theory Study of Boron Hydrides

Shan Xi Tian

Hefei National Laboratory for Physical Sciences at Microscale, Laboratory of Bond Selective Chemistry, Department of Chemical Physics, University of Science and Technology of China, Hefei, Anhui 230026, People's Republic of China

Received: January 5, 2005; In Final Form: April 20, 2005

Boron hydrides (BH_3, B_2H_6, B_3H_7, B_4H_{10}, B_5H_9, and B_5H_{11}) and their cations are studied by the coupled cluster CCSD(T) theory, the second-order Møller−Plesset (MP2) perturbation method, and the electron propagator theory in the partial third-order quasi-particle approximation, using the 6-311G(d,p) basis set. The vertical ionization potential energies are calculated, indicating an excellent agreement with the experimental data from photoelectron spectroscopy. Assignments to the experimental spectra are made on the basis of the present computational analyses. A significant Jahn−Teller effect on BH_3^+ leads to two states, $^2A_1$ and $^2B_2$, with the split energy of 0.14 eV. The triple and double B−H−B bridges are formed in $B_2H_6^+$ and *b*-$B_3H_7^+$, respectively. A new B−H−B bridge is formed while two B−B bonds are broken in $B_5H_{11}^+$. The Jahn−Teller effect lowers the symmetry of B_5H_9 (C_{4v}) to $B_5H_9^+$ (C_2) but slightly influences the structure of *ara*-B_4H_{10} (C_{2v}). The calculated properties of geometries, vibrational frequencies, and energies are compared with the experimental data available in the literatures.

I. Introduction

Boron hydrides, as the typical electron-deficient molecules, attract a great amount of interest from theoretical and experimental chemists.[1] By virtue of the extensive application in chemistry, the studies of geometrical and valence structures can provide impetus for discoveries of new species and reactions. Nuclear magnetic resonance (NMR),[1] electron diffraction,[2] X-ray diffraction (XRD),[3−5] electron spin resonance (ESR),[6] and Fourier transform infrared (FT-IR)[7] experiments show that many boron hydrides have higher symmetries. The thermodynamic properties of boron hydrides have been studied using electron impact,[8] thermal explosion,[9] and photoionization experiments,[10] and the theoretical calculations at the different levels.[11−14] The evaluation of accurate self-consistent-field (SCF) wave functions for these boron hydrides is the next more-sophisticated step to understand the complicated polyhedra and fragmentation processes.[13,15] Helium(I) and helium(II) photoelectron spectroscopy (PES) can directly supply the molecular orbital (MO) pictures.[16] The PES experiments have been conducted for boron hydrides such as diborane,[17] tetraborane-(10),[18] pentaborane(9),[18,19] decaborane(14),[15,18] and other higher boranes[18,19] (where the numbers in parentheses represent the number of H atoms). Ab initio work was also performed correspondingly to make the assignments to the spectra.[15b,16−19] However, there are several factors to be considered in the selection of the level of theory and basis sets. Much computational work on the electron-deficient boranes has shown that electron correlation methods are essential to predict energies[20] and geometries[21] that are in good agreement with the experimental data. Moreover, it has been demonstrated that the polarization functions on H atoms improved the description of the bridging H atoms in carboranes.[22] Thereby, the *p*-type polarization functions are necessary in the basis set for the H atoms.

The previous assignments to the spectra of boron hydrides were based on the SCF calculations and Koopmans' theorem.[16−19] This treatment is too cursory to compare the experimental data, although electron correlation was partially included in the ΔSCF + CISD(Q) calculations.[16e] Quasi-particle approximations in electron propagator theory[23] are convenient extensions of the Koopmans' theorem to calculate ionization potentials (IPs). In the quasi-particle approximation, electrons that have been assigned to canonical MOs are subject to a correlated, energy-dependent potential represented by the diagonal elements of the self-energy matrix while nondiagonal elements are neglected. Ortiz and co-workers demonstrated the reliability of the partial third-order (P3) quasi-particle theory in the prediction of the vertical IPs (IP_v) and electron affinities of the different types of closed-shell or open-shell molecules.[24] Electron correlation and orbital relaxation effects are considered in the P3 approximation. Each IP_v calculated with the electron propagator methods corresponds to a Dyson orbital, which is described by

$$\phi^{\text{Dyson}}(x_1) = N^{-1/2}\int \Psi^*_{\text{cation}}(x_2, x_3, x_4, ..., x_N) \times \Psi_{\text{neutral}}(x_1, x_2, x_3, x_4, ..., x_N)\, dx_2\, dx_3\, dx_4 ... dx_N \quad (1)$$

where N is the number of electrons in the molecule and x_i is the space-spin coordinate of electron i. The Dyson orbital corresponding to each IP in the P3 approximation is proportional to a canonical, Hartree−Fock (HF) orbital. The pole strength is equal to the integral over all space of the absolute value squared of the Dyson orbital, indicating the perturbation to the results of Koopmans' theorem. These approximations are validated only when pole strengths lie between 0.85 and unity.[24]

In this work, the boron hydrides (BH_3, B_2H_6, B_3H_7, B_4H_{10}, B_5H_9, and B_5H_{11}) at the low-lying states are investigated at the higher ab initio level, combined with the electron propagator theory in the P3 approximation. In regard to B_3H_7 isomers, they may be involved in the conversion between bis(diboranyl)-tetraborane (bis-B_4H_{10}) to arachno-tetraborane (*ara*-B_4H_{10}),[25a] and the cation has been observed as the fragment of the higher boranes.[25b] The other five *classical* structures of B_5H_9 will not

10.1021/jp050067e CCC: $30.25
Published on Web 05/28/2005

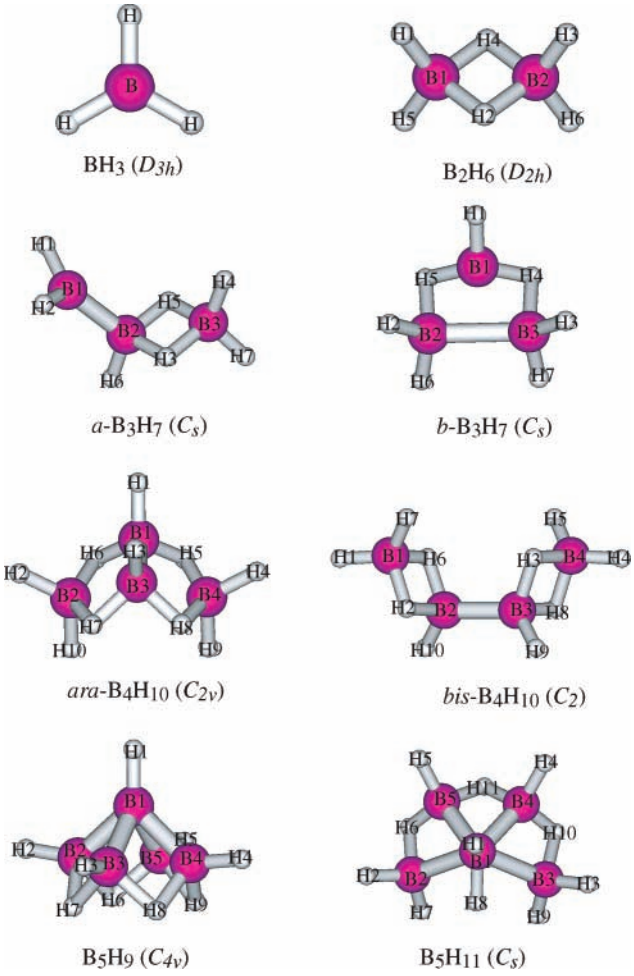

Figure 1. Optimized structures of the boron hydrides.

be considered in this work, because they are less stable, with respect to the *nonclassical* square pyramidal structure (C_{4v}).[11b] The Jahn−Teller effect was expected to occur for ionization processes of BH_3 (D_{3h}) and B_5H_9 (C_{4v}), because their highest occupied molecular orbitals (HOMOs) are the doubly degenerate 1e′ and 4e, respectively. Two split cationic states of BH_3^+ have been predicted to be $^2B_2$ and $^2A_1$;[12a] no studies extend to $B_5H_9^+$. The geometrical, vibrational, and energetic properties, the IP_v, and the adiabatic IP (IP_a) values will be compared with the experimental data available in the literature, which gives the insights of the characteristics of these electron-deficient molecules and may aid in the assignments of the spectra measured with higher-energy resolution.

II. Calculation Details

Ab initio calculations were performed with Gaussian 98.[26] Eight stable conformers in Figure 1 were optimized at the second-order Møller−Plesset (MP2) perturbation (frozen) level,[27] using the 6-311G(d,p) basis set, and were confirmed to be the local minima by evaluation of harmonic vibrational frequencies. All conformers besides B_5H_{11} were slightly away from the symmetries shown in Figure 1; however, it was found that those at the higher symmetries are more stable. The selected stable boron hydrides—BH_3, B_2H_6, *b*-B_3H_7, *ara*-B_4H_{10}, B_5H_9, and B_5H_{11}—were optimized for the lowest cationic states. No strong spin contamination was observed for the open-shell calculations. The single and double excitation coupled-cluster theory, including a perturbative estimate of triple excitations (CCSD(T)),[28] was applied in the extrapolated calculations over the MP2/6-311G(d,p) optimized geometries, to obtain the atomization energies of the neutral species (with respect to H ^2S and B ^2P) and the IP_a values. The IP_v values were predicted using the P3 approximation of the electron propagator theory and the 6-311G-(d,p) basis set.

All figures were produced by the MOLDEN graphics program.[29] The contour values in the MO electron density plots are equal to ±0.05.

III. Results and Discussion

A. Geometrical Parameters, Vibrational Frequencies, and Atomization Energies. The optimized geometrical parameters and dipole moments are listed in Table 1, in which the calculated results of BH_3 (D_{3h}), B_2H_6 (D_{2h}), *ara*-B_4H_{10} (C_{2v}), B_5H_9 (C_{4v}), and B_5H_{11} (C_s) are compared with the experimental data.[2−5,7,30−33] First, it is noted that there is some question about the symmetry of the pyramid-like B_5H_{11}. The energy at C_s symmetry is extremely similar to that at C_1 symmetry, although there is an imaginary vibrational frequency (i415.83 cm^{-1}) for the former. The previous studies predicted that the species at C_s symmetry was slightly unstable, with respect to the C_1 symmetry species.[11a,11e] The electron diffraction study also showed that the geometry of B_5H_{11} in the crystal was distorted from C_s symmetry in the gas phase.[2] The challenge is that the environment of the crystal and that of the isolated gas phase molecules modeled with theory are significantly different. Baerends and co-workers rebuilt the environment of the crystal by including a selection of ions or media molecules and concluded that the differences were largely due to charge effects.[34] The molecular potential energy surface of the pyramid-like B_5H_{11} for the B1−H8 wagging (see Figure 1) should be very flat. In the C_1 symmetric B_5H_{11}, the distance of H8 wagging from the C_s symmetry plane is ca. 0.1 Å, predicted at the MP2/6-311G-(d,p) level of theory. Such small geometrical distortion hardly affects the IPs and the other energetic properties. The C_s symmetry is adopted in the following discussion. Second, the terminal B−H bond lengths (except for the B1−H8 in the C_s symmetric B_5H_{11}) are found in a range of 1.182−1.195 Å; the bridging B−H bond lengths are in the range of 1.256−1.401 Å; the bridging B−H−B angles are in a range of 76.84°−87.65°; the B−B bond lengths are in the range of 1.691−2.010 Å. The aforementioned geometrical parameters are generally in good agreement with the experimental data.[2−5,7,30,31] Third, the calculated dipole moments of *ara*-B_4H_{10} (C_{2v}) and B_5H_9 (C_{4v}) are also in good agreement with the experiments.[32,33] Generally, the MP2/6-311G(d,p) calculations can predict the reliable geometrical parameters and wave functions of these boron hydrides.

Table 2 lists the harmonic vibrational frequencies, in comparison with the experimental data. The experimental infrared (IR) vibrational frequencies of BH_3,[30,35,36] B_2H_6,[37] and *ara*-B_4H_{10}[38] are available; however, the observed vibrational frequencies somehow are dependent on the experimental techniques. In particular, the ν_2 out-of-plane (E′ symmetry) bend for BH_3 was observed at 1140.9 cm^{-1} via diode laser IR spectroscopy[30] while at a wavenumber of 1125 cm^{-1} in the cryogenic argon-matrix IR spectroscopy.[35] The symmetries of the vibrational modes for B_2H_6 assigned previously[37] distinctly differ from the present assignments, which are the same as those given by Feller et al.[14b] The *NIST webBook* supplies data for the IR spectrum of *ara*-B_4H_{10}, but no assignments are available.[38] According to the calculated frequencies and the intensities, we tentatively assign two strong peaks at ca. 2480 cm^{-1} and ca. 2590 cm^{-1} in the spectrum[38] as the terminal B−H

TABLE 1: Geometrical Parameters and Dipole Moments of the Neutral Boron Hydrides

boron hydride	Geometrical Parameters: bond length (Å)	Geometrical Parameters: bond angle (deg)	dipole moment, μ (Debye)
BH_3 (D_{3h})	R(B−H) = 1.191 (1.185[a])	A(HBH) = 120.0	
B_2H_6 (D_{2h})	R(B1−H1) = 1.188 (1.184 ± 0.003,[b] 1.201[c]); R(B1−H2) = 1.316 (1.314 ± 0.003,[b] 1.320[c])	A(H1B1H5) = 122.2 (121.5 ± 0.5,[b] 121.0[c]); A(B1H2B2) = 84.42; D(H1B1H2H4) = 112.2	
a-B_3H_7 (C_s)	R(B1−H1) = 1.196; R(B1−B2) = 1.691; R(B2−H3) = 1.197; R(B2−H6) = 1.320; R(B3−H3) = 1.314; R(B3−H4) = 1.190	A(H1B1H2) = 116.5; A(B1B2H6) = 118.5; A(B2H3B3) = 84.35; A(H4B3H7) = 121.8; D(H1B1B2B3) = 91.79	0.112
b-B_3H_7 (C_s)	R(B1−H1) = 1.180; R(B1−H4) = 1.299; R(B2−B3)= 2.010; R(B2−H2) = 1.192; R(B2−H5) = 1.389; R(B2−H6) = 1.185	A(H1B1H4) = 115.1; A(B1H5B2) = 76.84; A(H2B2H6) = 120.1; A(H2B2B3) = 129.4; D(H2B2B3B1) = −82.36	1.222
ara-B_4H_{10} (C_{2v})	R(B1−H1) = 1.182(1.11 ± 0.04[d,e]); R(B1−H5) = 1.256(1.21 ± 0.03[d]); R(B1−B3) = 1.731 (1.750[d]); R(B2−H2) = 1.190; R(B2−H6) = 1.419 (1.37 ± 0.10[d]); R(B2−H10) = 1.195	A(H1B1H6) = 112.0; A(H1B1B3) = 114.6; A(B1H6B2) = 87.65; A(H2B2H6) = 104.3; A(H2B2H10) = 119.6; D(B1B2B3B4) = −52.97	0.523 (0.56[f])
bis-B_4H_{10} (C_2)	R(B1−H1) = 1.188; R(B1−H2) = 1.318; R(B1−H7) = 1.190; R(B2−H2) = 1.318; R(B2−H10) = 1.194; R(B2−B3) = 1.704	A(H1B1H2) = 109.2; A(H1B1H7) = 122.0; A(H2B2H10) = 106.8; A(H10B2B3) = 121.7; A(H2B2B3) = 110.6; D(B1B2B3B4) = −72.42	0.146
B_5H_9 (C_{4v})	R(B1−H1) = 1.179 (1.19[g]); R(B1−B2) = 1.702 (1.66[g]); R(B2−H2) = 1.183 (1.19[g]); R(B2−H6) = 1.348 (1.35[g])	A(H1B1B2) = 131.6; A(H2B2B1) = 132.0; A(H2B1H6) = 108.4; A(B2H7B3) = 83.87; A(B2B1B3) = 63.90; A(B1B2H6) = 105.2; D(B1B2B3B4) = −51.42	2.266 (2.13[h])
B_5H_{11} (C_s)	R(B1−H1) = 1.182 (1.19[i,e]); R(B1−B5) = 1.742 (1.72,[i,j] 1.77,[i,j] 1.742[k]); R(B1−H8) = 1.238 (1.19,[i,e] 1.327[k]); R(B1−B2) = 1.874 (1.85,[i] 1.892[k]); R(B2−H2) = 1.190 (1.19[i,e]); R(B2−H6) = 1.401 (1.34,[i] 1.594[k]); R(B2−H7) = 1.195 (1.19[i,e]); R(B5−H5) = 1.183 (1.19[i,e]); R(B5−H6) = 1.273 (1.274[k]); R(B5−H11) = 1.341 (1.32,[i] 1.334[k])	A(H1B1H8) = 116.9; A(H1B1B2) = 122.6; A(B2B1B5) = 59.20; A(B2B1B3) = 107.3; A(B2H6B5) = 83.88; A(B4B1B5) = 62.25; A(B4H11B5) = 84.36; A(H2B2B1) = 115.0; A(H5B5B1) = 120.6; D(B1B2B3B4) = −60.46	1.769

[a] From ref 35. [b] From ref 7. [c] From ref 31. [d] From ref 3. [e] Mean value of the B−H(terminal) lengths. [f] From ref 32. [g] From ref 4. [h] From ref 33. [i] From ref 5. [j] The C_1 symmetry was found in the crystalline form. [k] From ref 2.

vibrations (mainly 2620.4 cm^{-1}, A_1; 2617.6 cm^{-1}, B_2; 2714.3 cm^{-1}, A_1; cm^{-1}, A_1; 2714.9 cm^{-1}, B_2; 2735.3 cm^{-1}, B_1; 2743.5 cm^{-1}, A_1). The bridging H vibrations (2299.9 cm^{-1}, B_2; 2276.3 cm^{-1}, B_1; 2272.5 cm^{-1}, A_1; 1589.9 cm^{-1}, A_1; 1540.0 cm^{-1}, B_1) can be assigned to the peak at ca. 2140 cm^{-1} and several peaks in a range of 1400∼1600 cm^{-1} in the spectrum.[38] It is interesting to investigate the locally bridging H vibrations in the other boron hydrides. There is only one vibration at 1763.2 cm^{-1} (B_{3u}) in B_2H_6. It is slightly red-shifted (1737.8 cm^{-1}, A′) in *a*-B_3H_7; whereas it is split into more peaks for *b*-B_3H_7, B_5H_9, and B_5H_{11}. There are four vibrations in *b*-B_3H_7 (1482.4 and 2158.1 cm^{-1} (A″), 1548.3 cm^{-1} (A′), and 2097.4 cm^{-1} (A′)), five vibrations in B_5H_9 (2013.0 cm^{-1}(A_1), 1973.0 cm^{-1} (B_1, IR inactive), 1711.4 cm^{-1} (B_2, IR inactive), and 1578.7 cm^{-1} (E, doubly degenerate) and 1975.7 cm^{-1} (E, doubly degenerate)), two vibrations in bis-B_4H_{10} (1766.4 cm^{-1} (A) and 1718.8 cm^{-1} (B)), and six vibrations in B_5H_{11} (1538.5, 1999.4, and 2195.3 cm^{-1} (A′) and 1517.2, 1617.2, and 2187.0 cm^{-1} (A″)). Moreover, these vibrations have relatively large intensities, which can be the fingerprints for each species in the IR spectra.

In addition to the frequency shifts or splits, in comparison with the experimental data, the atomization energies provide the quantitative measure of the thermodynamic stability for each species. The experimental data of BH_3, B_2H_6, *ara*-B_4H_{10}, B_5H_9, and B_5H_{11} are from the thermal explosion,[9] the photoionization experiments,[10] and the JANAF tables.[39] The atomization energies for each species, together with the experimental data, are gathered in Table 3. The zero-point vibrational energy (ZPVE) corrections are included without scaling. The MP2 and the extrapolated CCSD(T) results match the experimental data well, except that for B_5H_{11}. The calculated results for B_5H_{11} are larger by ca. 0.5 au than the experimental datum (−1.954 au).[9] Moreover, one may notice that the MP2 results, including the ZPVE corrections, are much smaller than the experimental data, whereas those without the ZPVE corrections are more similar to the experimental data.

B. Vertical Ionization Potentials and Assignments to the Photoelectron Spectra. *1. BH_3 and B_2H_6.* The IP_v values of BH_3 and B_2H_6 obtained by the P3 electron propagator theory calculations, as well as the experimental data, are listed in Table 4. Although no PES of BH_3 was reported, a broad ionization band was predicted at the low IP energy, because of the strong Jahn−Teller effect, implying a wide Franck−Condon range.[12a] The IP_v, as well as IP_a, is not easy to determined from the experiments, which is similar to the case of methane.[40] Fehlner and Koski reported an ionization energy of IP = 11.4 ± 0.2 eV,[8a] whereas Wilson and McGee gave a value of 12.32 ± 0.1 eV via electron impact.[8b] The IP_v values for $1e'^{-1}$ and $2a_1'^{-1}$ states are predicted to be 12.986 and 18.106 eV, respectively, by the P3 electron propagator theory calculations. The electron density plots for these two MOs have been shown in Figure 2a. The ground state of BH_3 has the following electron configuration: $^1A_1'$: $(1a_1')^2(2a_1')^2(1e')$.[4] The HOMO 1e′, which is the doubly degenerate MO, shows pseudo $\pi_{BH_2}^-$ characteristics, whereas $2a_1'$ shows the MO characteristics of the B 2s orbital.

The prior theoretical IP calculations beyond the Koopmans' theorem were performed for B_2H_6 with the Green's function method, which demonstrated the validity of the one-particle picture to describe the ionization processes for the valence orbitals.[41] The present calculated results are in good agreement with the PES data[17] in Table 4. Note that the conventional assignments to the spectrum were $1b_{2g}$, $3a_g$, $1b_{3u}$, $1b_{2u}$, and $2a_g$ in the IP energy sequence.[17,41] The present calculated IP_v values

TABLE 2: Harmonic Vibrational Frequencies of the Neutral Boron Hydrides, in Comparison with the Experimental Data

boron hydride	harmonic vibrational frequencies (cm^{-1})
BH_3 (D_{3h})	A_2'': 1178.9 (1125,[a] 1140.9[b]) E': 1239.0 (1604[a]), 2734.4 (2808,[a] 2601.6[b]) A_1': 2598.0
B_2H_6 (D_{2h})	B_{2u}: 358.17 (368[c]), 981.64 (950[c]), 2756.5 (2612[c]) A_g: 822.35 (794[c]), 1230.1 (1180[c]), 2210.5 (2104[c]), 2661.2 (2524[c]) A_u: 867.84 (833[c]) B_{2g}: 904.25 (850[c]), 1926.1 (1768[c]) B_{1g}: 952.72 (915[c]), 2743.1 (2591[c]) B_{1u}: 1010.2 (973[c]), 2023.1 (1915[c]) B_{3g}: 1084.1 (1012[c]) B_{3u}: 1217.6 (1177[c]), 1763.2 (1602[c]), 2645.7 (2525[c])
a-B_3H_7 (C_s)	A':165.87, 513.37, 676.70, 900.00, 955.57, 1002.7, 1124.8, 1227.4, 1251.0, 1737.8, 2205.1, 2609.9, 2629.4, 2645.0, 2737.9 A'': 232.81, 367.63, 763.69, 908.62, 965.47, 1058.4, 1900.3, 2027.8, 2683.0
b-B_3H_7 (C_s)	A'': 282.96, 693.03, 854.49, 880.09, 982.77, 1108.6, 1195.7, 1482.4, 2158.1, 2739.1, 2637.4 A': 444.68, 654.20, 717.77, 804.91, 939.53, 985.21, 1085.3, 1231.4, 1548.3, 2097.4, 2645.9, 2753.2, 2769.6
ara-B_4H_{10} (C_{2v})[d]	A_1: 233.84, 591.36, 697.47, 816.11, 865.78, 1024.2, 1202.7, 1585.9, 2272.5, 2620.4, 2714.3, 2743.5 A_2: 418.01, 698.52, 936.62, 1047.6, 1109.3, 1500.1, 2317.2 B_1: 591.22, 758.32, 937.13, 1030.3, 1124.1, 1540.0, 2276.3, 2735.3 B_2: 366.39, 527.93, 896.68, 953.93, 1183.8, 1353.5, 2299.9, 2617.6, 2714.9
bis-B_4H_{10} (C_2)	*A*: 74.590, 157.39, 456.77, 555.80, 722.74, 903.59, 912.22, 961.68, 963.48, 971.52, 1063.7, 1169.9, 1226.4, 1766.4, 1914.4, 2018.2, 2200.0, 2639.1, 2659.5, 2736.7 *B*: 202.43, 388.60, 671.73, 837.13, 896.22, 957.49, 1064.1, 1075.8, 1223.2, 1718.8, 1896.4, 2010.9, 2200.2, 2637.0, 2650.6, 2735.8
B_5H_9 (C_{4v})	A_1: 720.78, 820.50, 1016.9, 1186.4, 2013.0, 2747.9, 2766.8 A_2: 864.67, 1509.7 B_1: 617.01, 776.69, 1040.4, 1973.0 B_2: 487.77, 725.38, 808.02, 1711.4, 2735.5 *E*: 585.52, 641.86, 809.87, 905.55, 951.39, 1099.1, 1578.7, 1975.7, 2743.5
B_5H_{11} (C_s)	A': 291.69, 427.35, 483.71, 612.73, 640.44, 768.69, 787.93, 866.60, 898.32, 954.12, 1005.5, 1071.6, 1118.5, 1140.9, 1230.7, 1538.5, 1999.4, 2195.3, 2413.9, 2618.1, 2710.6, 2730.9, 2745.1 A'': *i*415.83, 214.27, 539.83, 637.11, 719.35, 753.17, 855.39, 912.69, 939.30, 957.89, 1051.8, 1085.7, 1214.7, 1517.2, 1671.5, 2187.0, 2610.9, 2707.2, 2735.0

[a] From ref 35. [b] From refs 30 and 36. [c] From ref 37. [d] From the IR spectrum taken from ref 38; see discussion in the text.

TABLE 3: Atomization Energies of the Neutral Boron Hydrides, in Comparison with the Experimental Data

	Atomization Energy (au)		
boron hydride	MP2[a]	CCSD(T)	experimental data
BH_3 (D_{3h})	−0.4259 (−0.3992)	−0.4283	−0.423,[b] −0.444[c]
B_2H_6 (D_{2h})	−0.9190 (−0.8548)	−0.9216	−0.917,[d] −0.967[c]
a-B_3H_7 (C_s)	−1.1710 (−1.0952)	−1.1679	
b-B_3H_7 (C_s)	−1.1865 (−1.1097)	−1.1811	
ara-B_4H_{10} (C_{2v})	−1.6790 (−1.5667)	−1.6698	−1.670[d]
bis-B_4H_{10} (C_2)	−1.6637 (−1.5515)	−1.6600	
B_5H_9 (C_{4v})	−1.8150 (−1.7077)	−1.7830	−1.800[d]
B_5H_{11} (C_s)	−2.4681 (−2.3438)	−2.4478	−1.954[d]

[a] The values in parentheses represent atomization energies obtained with the zero-point-vibrational energy corrections. [b] From ref 10. [c] From ref 39. [d] From ref 9.

are somewhat more similar to the experimental data than the Green's function results[41] for the first two ($1b_{1g}^{-1}$ and $3a_g^{-1}$) and last two ($2b_{3u}^{-1}$ and $2a_g^{-1}$) bands. Similar work was performed at the P3 or NR2/6-311G(2df,2pd)//MP2 /6-311G-(2d,p) level, where NR2 was an extension version of the P3 method.[24c] As shown in Table 4, the P3/6-311G(2df,2pd) results are slightly larger than the present IP_v values, because of the inclusion of more polarization functions in the basis sets. On the other hand, the P3 approximation or the one-particle approximation may be invalid in the higher IP_v bands, because of the smaller pole strength (0.84 for $2a_g^{-1}$). In fact, a weak band at $IP_v \approx 19$ eV[17a,17b,17c] may be assigned to the electron correlation effect. Namely, a shake-up (HOMO($1b_{1g}$) → LUMO, where LUMO is the lowest unoccupied molecular orbital, $1b_{2g}$) correlates with the ionization $1b_{1g}^{-1}$, according to the weak transition observed as $1b_{1g} \rightarrow 1b_{2g}$ at 6.8 eV.[42] The other two strong transitions at 9.2 and 10.3 eV may be included in the $2a_g^{-1}$ band.[42] 2ph-TDA calculations predicted a series of lines at an IP_v value of ∼26−29 eV.[17d] The first ionization of B_2H_6 is from the $1b_{1g}$ orbital. In Figure 2b, this orbital, which is an antibonding orbital between the hydrogens, is located on the terminal B−H bonds and assigned as $\pi_{BH_2}^-$. In contrast to this orbital, the $1b_{2u}$ orbital is of the $\pi_{BH_2}^+$ type. The $3a_g$ and $1b_{1u}$ orbitals show the bridging B−H−B bonding characteristics (composed of B 2p and H 1s orbitals). The $2b_{3u}$ orbital is composed of B 2s and H 2p, whereas $2a_g$ is purely composed of B2s orbitals.

2. a-B_3H_7 and b-B_3H_7. The *b*-B_3H_7 isomer is more stable (by 8.28 kcal/mol) than the *a*-B_3H_7 isomer at the CCSD(T)//MP2 level. The calculated IP_v values for both of these isomers are given in Table 5; however, no experimental data are available. The electron density plots of the MOs of *b*-B_3H_7 are shown in Figure 3. The σ_{B-B} bond, 9a′ of *a*-B_3H_7 or 7a′ of *b*-B_3H_7, corresponds to an IP_v value of 10.69 or 11.31 eV. The Coulomb repulsion should be stronger between the σ_{B-B} bond (composed of B 2p and B 2p orbitals) and the residual part (similar to diborane) in *a*-B_3H_7 than that in *b*-B_3H_7, resulting in the smaller IP_v value of *a*-B_3H_7 (10.69 eV). The smaller pole strengths are predicted for the inner ionization states, indicating the possibility of satellites in the spectra.

3. ara-B_4H_{10} and bis-B_4H_{10}. The PES of tetraborane was assigned using *ara*-B_4H_{10}, in which the symmetries differed from

TABLE 4: Vertical Ionization Potentials of BH_3 and B_2H_6 in Comparison with the Experimental Data

boron hydride	orbital assignment	Vertical Ionization Potential, IP_v (eV) theoretical[a]	experimental
BH_3 ($^1A_1'$)	$1e'$	12.99 (0.93)	12.32,[e] 11.4[f]
	$2a_1'$	18.11 (0.91)	
B_2H_6 (^1A_g)	$1b_{1g}$	12.01 (0.92), 11.87 (0.94),[b] 12.13 (0.92),[c] 12.06 (0.91)[d]	11.89,[g] 11.81,[h] 11.88[i]
	$3a_g$	13.26 (0.92), 13.11 (0.93),[b] 13.40 (0.91),[c] 13.33 (0.90)[d]	13.30,[e] 13.3,[f] 13.35[i]
	$1b_{2u}$	13.74 (0.91), 13.73 (0.93),[b] 13.89 (0.91),[c] 13.80 (0.89)[d]	13.91,[e] 13.9,[f] 13.93[i]
	$1b_{1u}$	14.48 (0.92), 14.49 (0.93),[b] 14.66 (0.91),[c] 14.60 (0.91)[d]	14.75,[e] 14.7,[f] 14.76[i]
	$2b_{3u}$	16.10 (0.90), 16.21 (0.92),[b] 16.21 (0.90),[c] 16.02 (0.87)[d]	16.11,[e] 16.06,[f] 16.08[i]
	$2a_g$	21.85 (0.84), 22.33 (0.87),[b] 21.98 (0.84),[c] 21.42 (0.74)[d]	21.4,[f] 21.42[i]

[a] Pole strengths are given in parentheses. [b] Calculated by the Green's function method.[41] [c] The P3/6-311G(2df,2pd)//MP2/6-311G(2d,p) results.[24c] [d] The NR2/6-311G(2df,2pd)//MP2/6-311G(2d,p) results.[24c] [e] From ref 8a. [f] From ref 8b. [g] From ref 17a. [h] From ref 17b. [i] From ref 17e.

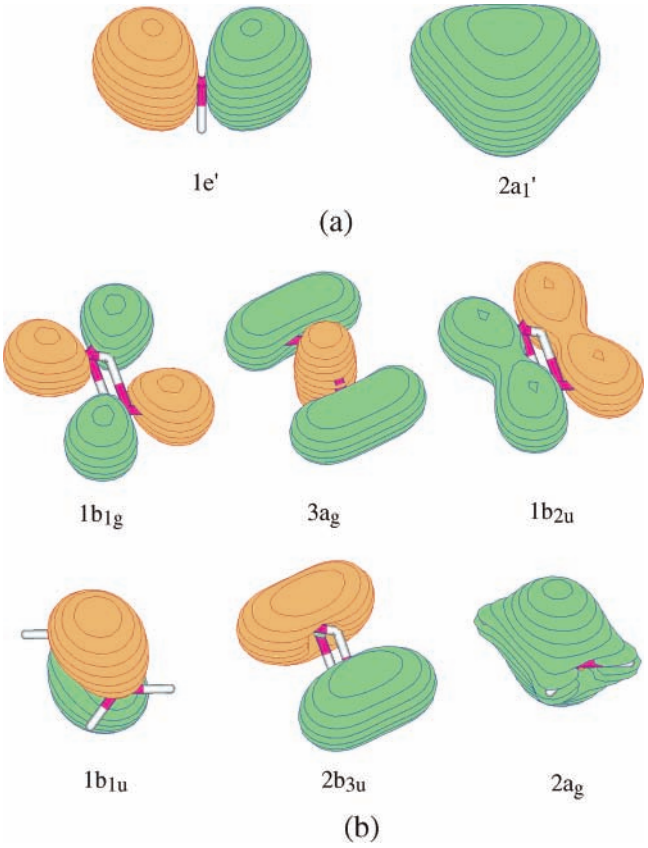

Figure 2. Electron density plots of the valence molecular orbitals (MOs) of (a) BH_3 and (b) B_2H_6.

the present ones from the third band.[8] The ground state of *ara*-B_4H_{10} has the following electron configuration: $^1A_1$: (core)^8 $(3a_1)^2$ $(2b_2)^2$ $(2b_1)^2$ $(4a_1)^2$ $(1a_2)^2$ $(5a_1)^2$ $(3b_2)^2$ $(3b_1)^2$ $(6a_1)^2$ $(4b_2)^2$ $(7a_1)^2$. The predicted IP_v values of *ara*-B_4H_{10}, as well as those for bis-B_4H_{10}, are compared with the PES analysis in Table 6, indicating a good agreement, except for the $3b_1^{-1}$, $6a_1^{-1}$, and $2b_1^{-1}$ states. In the spectrum, the $3b_1^{-1}$ and $6a_1^{-1}$ bands are seriously overlapped.[8] It is difficult to assign an accurate IP_v value to each band. The $2b_1^{-1}$ corresponds to a diffuse band, in which the first peak appears at 18.1 eV and the middle of the band is estimated to be located at ca. 18.4 eV.[8] Thereby, it is reasonable that the IP_v for $2b_1^{-1}$ is predicted to be 18.55 eV. The satellites corresponding to the shake-up or shake-off states are expected to be in the spectrum, because of the nonzero background at the higher IP_v region in the spectrum[8] and the smaller pole strengths (0.84 for $4a_1^{-1}$ and 0.78 for $2b_2^{-1}$) calculated in the P3 approximation.

Figure 4 presents the electron density plots of the MOs of the more stable *ara*-B_4H_{10}, to elucidate the molecular electronic structure and ionization process. The first ionization bands both for *ara*-B_4H_{10} and bis-B_4H_{10} are from the B−B bond. The IP_v of $7a_1$ (*ara*-B_4H_{10}) (11.44 eV) is higher than that of 8a (bis-

TABLE 5: Vertical Ionization Potential (IP_v) Values of B_3H_7

orbital assignment	theoretical IP_v[a] (eV)
a-B_3H_7 ($^1A'$)	
$9a'$	10.69 (0.91)
$2a''$	12.32 (0.92)
$8a'$	12.66 (0.91)
$7a'$	13.40 (0.91)
$1a''$	14.51 (0.91)
$6a'$	15.36 (0.90)
$5a'$	17.41 (0.88)
$4a'$	21.59 (0.82)
b-B_3H_7 ($^1A'$)	
$7a'$	11.31 (0.91)
$4a''$	11.78 (0.91)
$6a'$	12.89 (0.90)
$3a''$	13.25 (0.90)
$5a'$	14.16 (0.89)
$4a'$	15.95 (0.88)
$2a''$	17.85 (0.86)
$3a'$	21.77 (0.80)

[a] Pole strengths are given in parentheses.

TABLE 6: Vertical Ionization Potential (IP) Values of B_4H_{10}, in Comparison with the Experimental Data

orbital assignment	IP_v (eV) theoretical[a]	experimental[b]
	ara-B_4H_{10} ($^1A_1$)	
$7a_1$	11.44 (0.91)	11.5
$4b_2$	12.15 (0.91)	12.1
$6a_1$	12.47 (0.90)	12.62
$3b_1$	12.48 (0.90)	12.93
$3b_2$	14.07 (0.90)	14.12
$5a_1$	14.38 (0.90)	14.52
$1a_2$	15.87 (0.88)	15.84
$4a_1$	18.55 (0.84)	18.1
$2b_1$	19.16 (0.86)	18.9
$2b_2$	22.66 (0.78)	23.1
	bis-B_4H_{10} (^1A)	
8a	10.54 (0.90)	
7b	12.20 (0.91)	
7a	12.78 (0.91)	
6b	13.03 (0.91)	
6a	13.33 (0.90)	
5a	14.32 (0.90)	
5b	14.45 (0.90)	
4b	15.18 (0.89)	
4a	16.07 (0.88)	
3b	21.04 (0.84)	

[a] Pole strengths are given in parentheses. The present assignments to the spectrum are different from those given previously. [b] From ref 18.

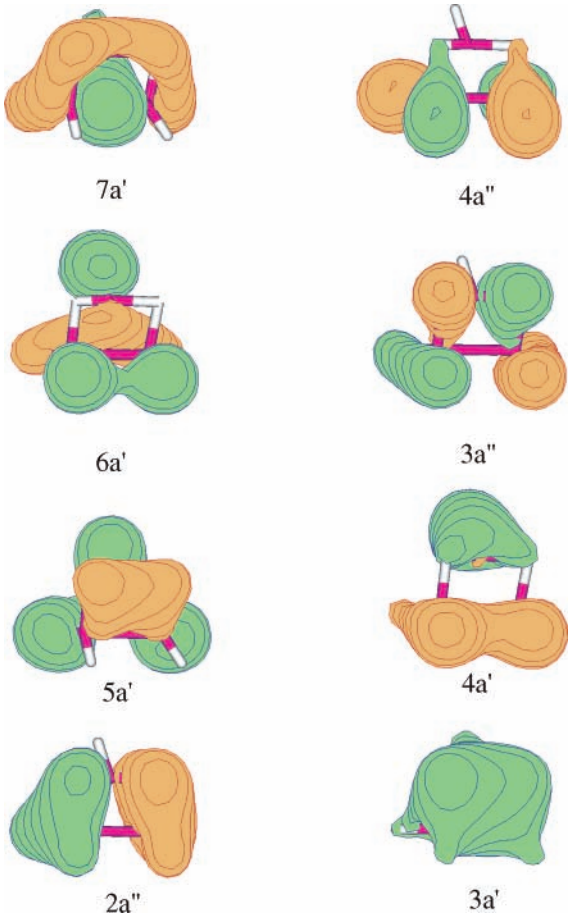

Figure 3. Electron density plots (top-viewed) of the valence MOs of *b*-B_3H_7.

B_4H_{10}), indicating that the *nonclassical* (ringlike *b*-B_3H_7 or polyhedral *ara*-B_4H_{10}) structures are more stable than the *classical* ones (*a*-B_3H_7 and bis-B_4H_{10}).[11] The next HOMOs ($4b_2$, $6a_1$, $3b_1$, $3b_2$, and $4a_1$) of *ara*-B_4H_{10} are of the terminal B−H bonds, whereas $5a_1$ and $1a_2$ are of the bridging B−H−B bonds. The last three MOs mainly show the B 2s characteristics.

4. B_5H_9 and B_5H_{11}. The PES of B_5H_9 and B_5H_{11} were recorded by Lloyd et al.[18] and Fehlner and co-workers.[19] The detailed assignments to the spectrum of B_5H_9 were made by Lloyd et al.,[18] which is in good agreement with the present work. In Table 7, the IP_v values as well as the pole strengths are listed for B_5H_9 and B_5H_{11}, in comparison with the experimental data.[18,19] To the best of our knowledge, as far as these two molecules are concerned, there are no theoretical IP calculations prior to this work beyond the Koopmans' theorem. The ground state of B_5H_9 has the following electron configuration: $^1A_1$: $(core)^{10}$ $(3a_1)^2(2e)^4(4a_1)^2(2b_2)^2(5a_1)^2(1b_1)^2(3e)^4(6a_1)^2(4e)$.[4] It is noted that the energy sequence at the Koopmans' approximation ($1b_1^{-1}$, $5a_1^{-1}$, and $2b_2^{-1}$) is changed in the P3 approximation to be $1b_1^{-1}$, $1b_2^{-1}$, and $5a_1^{-1}$. The scaled Koopmans' results[18] happened to give the same sequence as the P3 calculations. In fact, the dynamic electron correlation and relaxation effects are important to predict the corrected IP_v values. Moreover, these three bands are seriously overlapped, and the experimental IP_v data are not as reliable as the other bands.[18] Only the peak position (14.6 eV) was given in the other experimental work.[19]

The more-complex spectrum of B_5H_{11}[19] makes assignments rather difficult. The IP_v values predicted by the P3 calculations are in good agreement with the experimental data. The sequence between 10a′ and 6a″ at the Koopmans' approximation is reversed in the P3 approximation; however, only one band was observed for these two MOs.[19] The experimental spectrum of B_5H_{11} was only extended to ca. 15 eV; no higher IP bands were reported.[19] The calculations are performed to the inner ionization state $4a'^{-1}$. Smaller pole strengths for the inner three states both for B_5H_9 and B_5H_{11} are observed, indicating again the invalidity of the P3 approximation for the inner ionization states.

TABLE 7: Vertical Ionization Potential (IP_v) Values of B_5H_9 and B_5H_{11}, in Comparison with the Experimental Data

	Vertical Ionization Potential, IP_v (eV)	
orbital assignment	theoretical[a]	experimental
	B_5H_9 ($^1A_1$)	
4e	10.41 (0.90)	10.53,[b] 10.5[c]
$6a_1$	12.07 (0.90)	12.27,[b] 12.2[c]
3e	12.68 (0.90)	12.56,[b]12.7[c]
$1b_1$	14.25 (0.89)	14.33[b]
$5a_1$	14.55 (0.88)	14.83,[b] 14.6[c]
$2b_2$	14.53 (0.89)	14.59,[b]
$4a_1$	16.55 (0.84)	16.38,[b] 16.4[c]
2e	18.85 (0.84)	18.37,[b]18.6[c]
$3a_1$	23.38 (0.67)	23.2[b]
	B_5H_{11} ($^1A'$)	
7a″	10.74 (0.90)	10.7[c]
11a′	11.61 (0.90)	11.7[c]
10a′	12.11 (0.90)	}12.2[c]
6a″	12.08 (0.90)	
9a′	12.65 (0.90)	12.5[c]
5a″	13.11 (0.90)	(13.1)[c]
8a′	13.91 (0.90)	14.0[c]
7a′	14.94 (0.88)	14.8[c]
4a″	15.00 (0.88)	
6a′	16.75 (0.85)	
5a′	18.76 (0.84)	
3a″	19.88 (0.83)	
4a′	22.78 (0.76)	

[a] Pole strengths are given in parentheses. [b] From ref 18. [c] From ref 19.

Figures 5 and 6 show the MO electron density plots of B_5H_9 and B_5H_{11}, respectively. The HOMO 4e of B_5H_9 is a doubly degenerate MO and shows the B−B bonding characteristics. The terminal B−H bonds are observed in the $6a_1$, 3e, and $2b_2$ orbitals. The $1b_1$, $5a_1$, and $4a_1$ orbitals show the characteristics of the bridging B−H−B bonds. The doubly degenerate MO 2e shows characteristics of the B 2s orbitals and the part of H 2p, while the inner $3a_1$ is purely composed of the B 2s orbitals. The first four MOs of B_5H_{11} present the B−B bonds and, partly, the terminal B−H bonds. The bridging B−H−B bonds can be found in the 5a″, 8a′, 7a′, and 6a′. 5a′ and 3a″ are composed of the B 2s and H 2p orbitals, and 4a′ is purely composed of the B 2s orbitals.

In regard to the systems in which the strong configuration interactions break down the single-particle model, the higher level of theory is applicable. As mentioned previously, the ionizations of the inner MOs of boron hydrides may show some satellites in the spectra. Moreover, the third-order algebraic-diagrammatic construction (ADC(3)) scheme for the one-particle Green's function[43] and the symmetry-adapted cluster configuration interaction (SAC−CI) method[44] can predict reliable IP_v values for both the valence ionization and the satellite states. The latter method was encoded in a recent version of the Gaussian program, and further studies of the ionization and excited states of boron hydrides using the SAC−CI method will be performed in our group. MO characteristics can be also rationalized by (e,2e) electron momentum spectroscopy[45a] and Penning ionization electron spectroscopy.[45b,45c] The unusual bonding in boron hydrides is worthy of further study, using the aforementioned theoretical and experimental methods.

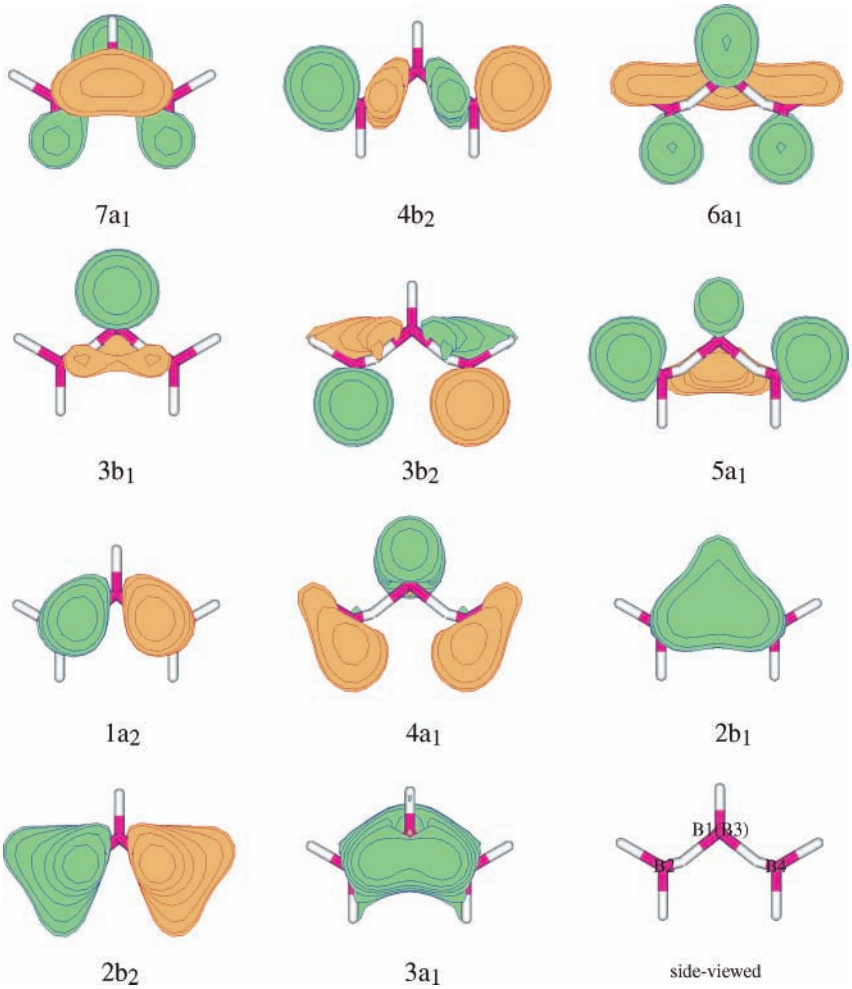

Figure 4. Electron density plots (side-viewed) of the valence MOs of *ara*-B_4H_{10}.

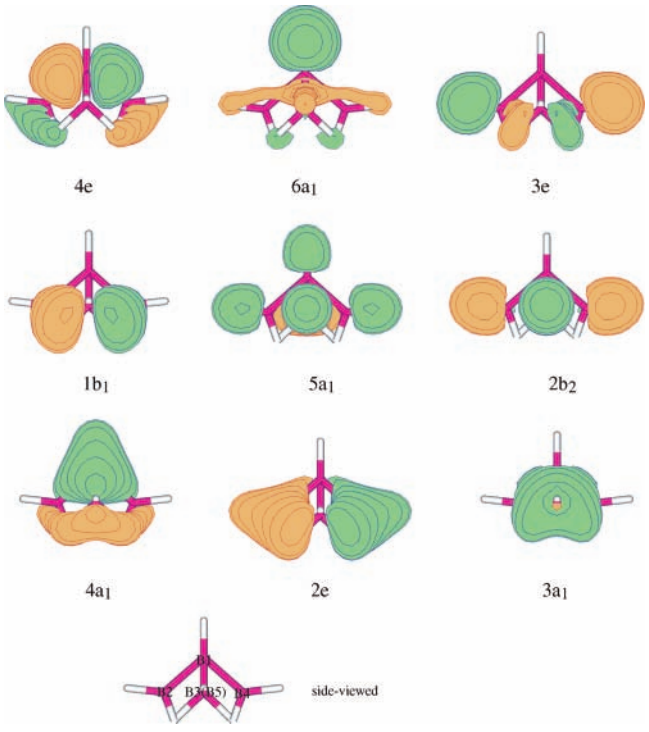

Figure 5. Electron density plots (side-viewed) of the valence MOs of B_5H_9.

C. Cations and Adiabatic Ionization Potentials. The IP_v values are calculated over the geometrical structure of the neutral species. The geometrical relaxation is closely correlated with the thermodynamic properties. As mentioned in the Introduction, the strong Jahn−Teller effect has been predicted for BH_3^+,[12a] and $B_2H_6^+$ was suspected to be a metatstable or short-lived state.[10,12b] It is full of meaning to study the cationic states of the boron hydrides. The optimized structures of BH_3^+, $B_2H_6^+$, *b*-$B_3H_7^+$, *ara*-$B_4H_{10}^+$, $B_5H_9^+$, and $B_5H_{11}^+$ are schemed in Figure 7, and the parameters are listed in Table 8. The IP_a values are obtained on the basis of the energetic calculations of these cations, and they are given in Table 9, in comparison with the experimental data.[8a,8c,10,12,17a,17b,17e,18,46,47]

1. BH_3^+. The MP2(full)/6-31G* calculations predicted bond lengths B−H of 1.164 and 1.266 Å and bond angles of 75.0° and 142.5° for the $^2A_1$ state of BH_3^+, and bond lengths of 1.171 and 1.574 Å and bond angles of 162.6° and 98.7° for the $^2B_2$ state of BH_3^+.[12a] The present MP2/6-311G(d,p) predicted slightly different geometrical parameters, because of the larger basis set. Thereby, the IP_a value that corresponds to the respective state differs slightly. The split energy due to the Jahn−Teller effect is predicted to be 0.14 eV at the CCSD(T)/6-311G(d,p)//MP2/6-311G(d,p) level, which is ∼0.13 eV, as obtained at the MP4/6-311G**/MP2(full)/6-31G* level.[12a] The experimental IP_a value was estimated to be 12.026 ± 0.024 eV,[10] which may correspond to the $^2A_1$ state.

2. $B_2H_6^+$. The geometrical parameters were ever optimized at the MP2(full)/6-31G* level and were observed to be a C_s symmetrical complex between $B_2H_5^+$ and H.[12b] The separation between the B and H atoms is 3.606 Å.[12b] However, such a complex is not found by the MP2/6-311G(d,p) calculations,

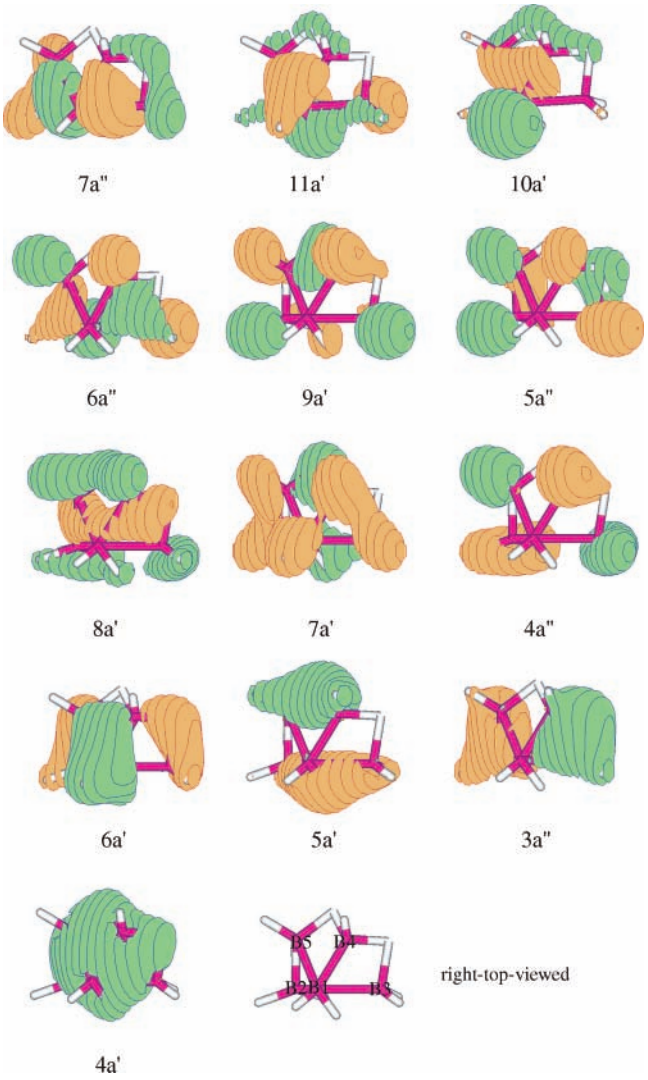

Figure 6. Electron density plots (right-top-viewed) of the valence MOs of B_5H_{11}.

because of the polarization p functions added to the basis set of the H atoms. During the optimization of $B_2H_6^+$, the distorted dibridged (C_{2v} symmetrical) structure[12b] was also found, but it has an imaginary vibrational frequency of *i*419.34 cm^{-1}, which is predicted at the MP2/6-311G(d,p) level. The C_s symmetrical structure in Figure 7 is located by the optimization along this imaginary vibrational mode. The bridging H atoms (H2 and H4) slightly shift to the B1 atom, and a weak B1−H3 bond is formed. This conformer actually relates to the $B_2H_5^+$ fragment, which is a triply bridged ion.[10,12b] $B_2H_6^+$ signal was extremely weak in the photoionization mass spectroscopy study, and it was 1000 times less abundant than $B_2H_5^+$.[10] The threshold potential for $B_2H_6 + h\nu \rightarrow B_2H_5^+ + H + e^-$ was deduced to be smaller than 11.40 ± 0.05 eV.[10] On the other hand, the measured IP_a value was 11.37 ± 0.05 eV,[10] 11.41 ± 0.02 eV,[17a] or 11.38 ± 0.01 eV.[17b] The previous electron impact value was 11.9 ± 0.1 eV,[8c] which may be due to the vibrational structure.[10] However, the recent experimental work gave the smaller IP_a value of 11.29 ± 0.01 eV.[17e] The present calculated results, 11.36 eV at the MP2/6-311G(d,p) level and 11.40 eV at the CCSD(T)/6-311G(d,p) level, are much better than the prior ones obtained at the MP4/6-311G(d,p)//HF/6-31G(d) level,[12b] which is in excellent agreement with the experimental data.[10,17a,17b] Moreover, the dissociation channel $B_2H_6^+ \rightarrow B_2H_5^+ + H$ correlates strongly with the potential surface of $B_2H_6^+$ ($^2A'$), which is the reason for this short-lived cationic state.

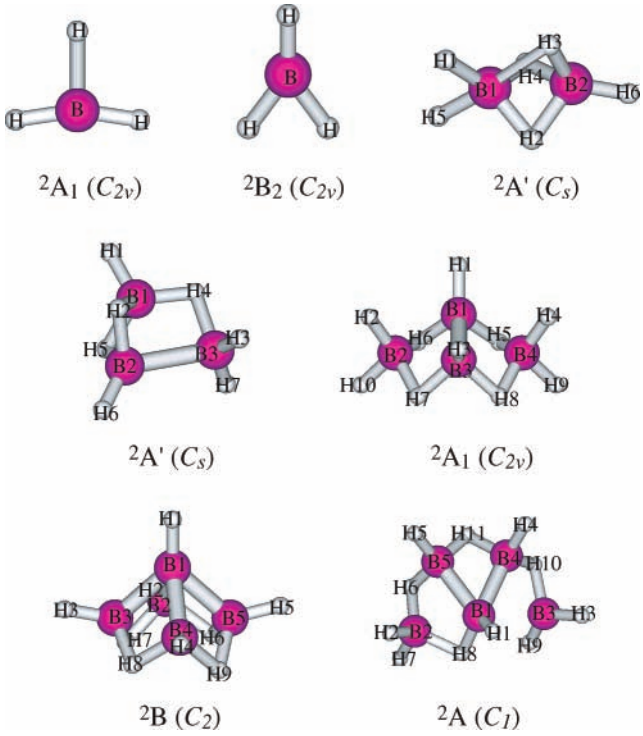

Figure 7. Optimized structures of the cations of boron hydrides.

3. b-$B_3H_7^+$. Double B−H−B bridges are formed in *b*-$B_3H_7^+$, because of the ionization that occurs on the part of the terminal B−H bond included in the HOMO of *b*-B_3H_7 (see Figure 3). The B2−H2 bond length is 1.339 Å, which is in the range of the normal B−H bridging bonds (1.256−1.401 Å). The IP_a is predicted to be 10.02 or 10.03 eV, whereas the threshold potential for $B_3H_7 + h\nu \rightarrow B_3H_6^+ + H + e^-$ was observed at 11.2 ± 0.3 eV.[46] Namely, *b*-$B_3H_7^+$ has the high thermodynamic stability and is detected in the experiment.[25b]

4. ara-$B_4H_{10}^+$. The first ionization mainly occurs on the σ_{B1-B3} bond ($7a_1$), thereby, the dihedral angle D(B1B2B3B4) is widened by 21.97°, with respect to the neutral and the species keeps the C_{2v} symmetry. The terminal B−H bonds are slightly elongated, because of their small distributions to $7a_1$ (see Figure 4). The IP_a is predicted to be 10.35 eV at the CCSD(T)/6-311G-(d,p) level, which is closer to the experimental value of 10.39 eV[8a] but less than 10.76 ± 0.04 eV.[18]

5. $B_5H_9^+$. The HOMO, 4e, is mainly of the σ_{B-B} bonds. The Jahn−Teller effect leads to the lower symmetrical (C_2) cation at the ^2B state. The cation with the higher symmetry (C_{2v}) appeared in the optimization but had an imaginary vibrational frequency of *i*560.32 cm^{-1}. There were no distinct split sub-bands observed in the first band.[18,19] The PES gave the IP_a at 9.87 ± 0.02 eV,[18] whereas the other experiments supplied data of 9.94 eV[47] and 9.90 eV.[48] The MP2 values are in good agreement with these data. The CCSD(T) calculations are beyond our computational ability for $B_5H_9^+$ and $B_5H_{11}^+$.

6. $B_5H_{11}^+$. Although the first ionization mainly occurs on the σ_{B-B} bonds, the strong mixing characteristics (both of σ_{B-B} bonds and the terminal B−H bonds) of 7a″ and the extremely long B1−H8 bond lead to H8 atom shifts to the B2 atom in the cation. The B1−B3 bond (2.089 Å) is weakened significantly, and finally a new B1−H8−B2 bridge is formed. The IP_a values that have been calculated at the MP2/6-311G(d,p) level are very similar to the PES datum (10.1 eV).[19]

TABLE 8: Geometrical Parameters of the Cationic Boron Hydrides

		Geometrical Parameters	
boron hydride	state	bond length (Å)	bond angle (deg)
BH_3^+ (C_{2v})	$^2A_1$	R(B−H) = 1.170, 1.269	A(HBH) = 145.9, 68.14
	$^2B_2$	R(B−H) = 1.181, 1.504	A(HBH) = 162.3, 98.87
$B_2H_6^+$ (C_s)	$^2A'$	R(B1−H1) = 1.242; R(B1−H2) = 1.311; R(B1−H3) = 1.675; R(B2−H2) = 1.357; R(B2−H3) = 1.258; R(B2−H6) = 1.171; R(B1−H5) = 1.276	A(H1B1H5) = 84.64; A(B1H2B2) = 72.66; A(B1H3B2) = 63.39; A(H6B2H3) = 128.2; D(H2B1H3B2) = 48.49
b-$B_3H_7^+$ (C_s)	$^2A'$	R(B1−H1) = 1.185; R(B1−H2) = 1.331; R(B2−B3) = 1.988; R(B2−H2) = 1.339; R(B1−H4) = 1.276; R(B3−H4) = 1.399; R(B3−H3) = 1.180	A(H1B1H2) = 108.6; A(B1H2B2) = 74.80; A(B1H4B3) = 97.18; A(H6B2B3) = 128.2; D(H2B2B3B1) = −47.48
ara-$B_4H_{10}^+$ (C_{2v})	$^2A_1$	R(B1−H1) = 1.176; R(B2−H2) = 1.200; R(B2−H10) = 1.217; R(B1−H6) = 1.340; R(B2−H6) = 1.316	A(H1B1B3) = 133.2; A(B1H6B2) = 86.06; A(H1B1H6) = 113.9; A(H2B2H10) = 108.2; A(H2B2H6) = 120.6; D(B1B2B3B4) = −31.00
$B_5H_9^+$ (C_2)	^2B	R(B1−H1) = 1.172; R(B1−B2) = 1.781; R(B1−B3) = 1.782; R(B2−H2) = 1.177; R(B2−H6) = 1.343	A(H1B1B2) = 132.9; A(H2B2B1) = 124.5; A(B3B1B2) = 57.91; A(B3B1B4) = 66.78; A(H2B2H6) = 109.1; A(B2H7B3) = 80.64; A(B3H8B4) = 93.77; D(B1B2B3B4) = −51.01
$B_5H_{11}^+$ (C_1)	^2A	R(B1−H1) = 1.179; R(B1−B4) = 1.819; R(B1−B5) = 1.834; R(B1−H8) = 1.304; R(B1−B2) = 1.859; R(B2−H2,7) = 1.197, 1.195; R(B2−H6) = 1.347; R(B2−H8) = 1.325; R(B3−H3,9) = 1.181, 1.183; R(B3−H10) = 1.355; R(B4−H4) = 1.178; R(B4−H10) = 1.290; R(B4−H11) = 1.345; R(B5−H5) = 1.176; R(B5−H6) = 1.307; R(B5−H11) = 1.315	A(H1B1H8) = 113.2; A(B4B1B5) = 57.57; A(B2H8B1) = 89.95; A(B2H6B5) = 90.26; A(B5H11B4) = 82.79; A(B4H10B3) = 88.82; A(H2B2H8) = 116.7; A(H5B5B1) = 123.0; D(B1B2B3B4) = −64.12

TABLE 9: Lowest Adiabatic Ionization Potentials of BH_3, B_2H_6, *b*-B_3H_7, *ara*-B_4H_{10}, B_5H_9, and B_5H_{11}, in Comparison with the Experimental Data

	Adiabatic Ionization Potential, IP_a (eV)					
	BH_3	B_2H_6	*b*-B_3H_7	*ara*-B_4H_{10}	B_5H_9	B_5H_{11}
			Theoretical[a]			
$^2B_2$:	11.89 (11.77)	11.36 (11.15)	10.03 (9.97)	10.42 (10.25)	9.92 (9.86)	9.94 (9.89)
	11.97[b]	11.40[b]	10.02[b]	10.35[b]		
	11.93[c]	11.30(11.28)[d]				
$^2A_1$:	12.02 (11.83)					
	12.11[b]					
	12.09[c]					
			Experimental			
	12.026 ± 0.024[e]	11.37 ± 0.05[e]		10.39[j]	9.94[l]	10.1[n]
		11.38 ± 0.01[f]		10.76 ± 0.04[k]	9.90[m]	
		11.41 ± 0.02[g]			9.87 ± 0.02[k]	
		11.9 ± 0.1[h]				
		11.29 ± 0.01[i]				

[a] The values given in parentheses are obtained at the (U)MP2/6-311G(d,p) level, including the zero-point-vibrational energy corrections. [b] The results obtained at the (U)CCSD(T)/6-311G(d,p)//(U)MP2/6-311G(d,p) level. [c] The MP4/6-311G(d,p)//HF/6-31G(d) results.[12a] [d] The MP4/6-311G**//MP2(full)/6-31G* results.[12b] [e] From ref 10. [f] From ref 17b. [g] From ref 17a. [h] From ref 8c. [i] From ref 17e. [j] From ref 8a. [k] From ref 18. [l] From ref 47. [m] From ref 48. [n] From ref 19.

IV. Conclusion

The neutral and cationic boron hydrides—BH_3, B_2H_6, *a*-B_3H_7, *b*-B_3H_7, *ara*-B_4H_{10}, bis-B_4H_{10}, B_5H_9, and B_5H_{11}—are studied at the high ab initio levels, MP2 and CCSD(T), using the 6-311G(d,p) basis set. The predicted properties of geometries, vibrational frequencies, and energies are compared with the experimental data that are available in the literature.

The P3 electron propagator theory is used to calculate the vertical ionization potential (IP_v) values. Photoelectron spectra of B_2H_6, B_4H_{10}, B_5H_9, and B_5H_{11} are re-assigned on the basis of the P3 calculations and the molecular orbital (MO) electron density plots. Generally, the P3 results are in excellent agreement with the experimental data. They will be of utmost importance to make assignments to the high-resolution spectra in the future. However, the inner ionization states are predicted to have the smaller pole strengths in the P3 approximation, indicating that the theoretical IP calculations at the higher levels meet the requirements of the analyses of the higher IP bands in the photoelectron spectroscopy.

A significant Jahn−Teller effect on BH_3^+ leads to two states—$^2A_1$ and $^2B_2$—with the split energy of 0.14 eV. There are triple B−H−B bridges in $B_2H_6^+$. Ionization also induces to the formation of the double B−H−B bridges in *b*-$B_3H_7^+$ and a new B−H−B bridge in $B_5H_{11}^+$. The Jahn−Teller effect lowers the symmetry of B_5H_9 (C_{4v}) to $B_5H_9^+$ (C_2), but slightly influences the structure of *ara*-B_4H_{10}. The aforementioned geometrical changes are interpreted by the MO electron density plots.

Acknowledgment. This work is partially supported by the Fund for the Young Research Fellows at University of Science and Technology of China. The author thanks the referees, who gave the valuable comments on the manuscript. Prof. J. V. Ortiz at Kansas State University is acknowledged for providing a copy of ref 24c.

References and Notes

(1) (a) Lipscomb, W. N. *Boron Hydrides*; W. A. Benjamin, Inc.: New York, 1963. (b) Shore, S. G. *Boron Hydride Chemistry*; Muetterties, E. L., Ed.; Academic Press: New York, 1975. (c) Onak, T. *Comprehensive Organometallic Chemistry*; Wilkinson, G., Stone, F. G. A., Abel, E., Eds.; Pergamon: Oxford, England, 1982.

(2) Greatrex, R.; Greenwood, N. N.; Rankin, D. W. H.; Robertson, H. E. *Polyhedron* **1987**, *6*, 1849.

(3) Nordman, C. E.; Lipscomb, W. N. *J. Chem. Phys.* **1953**, *21*, 1856.

(4) Dulmage, W. J.; Lipscomb, *Acta Crystallogr.* **1952**, *5*, 260.

(5) Lavine, L. R.; Lipscomb, W. N. *J. Chem. Phys.* **1954**, *22*, 614.

(6) (a) Catton, R. C.; Symons, M. C. R.; Wardale, H. W. *J. Chem. Soc. A* **1969**, 2622. (b) Sprague, E. D.; Williams, F. *Mol. Phys.* **1971**, *20*, 375.

(7) Duncan, J. L.; Harper, J. *Mol. Phys.* **1984**, *51*, 371, and references therein.

(8) (a) Fehlner, T. P.; Koski, W. S. *J. Am. Chem. Soc.* **1964**, *86*, 2733. (b) Wilson, J. H.; McGee, H. A., Jr. *J. Chem. Phys.* **1967**, *46*, 1444. (c) Koski, W. S.; Kaufman, J. J.; Pachucki, C. F.; Shipko, F. J. *J. Am. Chem. Soc.* **1958**, *80*, 3202.

(9) Gunn, S. R.; Green, L. G. *J. Phys. Chem.* **1961**, *65*, 2173.

(10) Ruščić, B.; Mayhew, C. A.; Berkowitz, J. *J. Chem. Phys.* **1988**, *88*, 5580.

(11) (a) McKee, M. L.; Lipscomb, W. N. *Inorg. Chem.* **1981**, *20*, 4442. (b) McKee, M. L.; Lipscomb, W. N. *J. Am. Chem. Soc.* **1982**, *21*, 2846. (c) McKee, M. L.; Lipscomb, W. N. *Inorg. Chem.* **1985**, *24*, 765. (d) McKee, M. L. *Inorg. Chem.* **1986**, *25*, 3545. (e) McKee, M. L. *J. Phys. Chem.* **1989**, *93*, 3426.

(12) (a) Curtiss, L. A.; Pople, J. A. *J. Phys. Chem.* **1988**, *92*, 894. (b) Curtiss, L. A.; Pople, J. A. *J. Chem. Phys.* **1988**, *89*, 4875.

(13) (a) Switkes, E.; Stevens, R. M.; Lipscomb, W. N.; Newton, M. D. *J. Chem. Phys.* **1969**, *51*, 2085. (b) Switkes, E.; Epstein, I. R.; Tossell, J. A.; Stevens, R. M.; Lipscomb, W. N. *J. Am. Chem. Soc.* **1970**, *92*, 3837.

(14) (a) Duke, B. J.; Gauld, J. W.; Schaefer, H. F., III. *J. Am. Chem. Soc.* **1995**, *117*, 7753. (b) Feller, D.; Dixon, D. A.; Peterson, K. A. *J. Phys. Chem. A* **1998**, *102*, 7053.

(15) Guest, M.; Hiller, I. H. *J. Chem. Soc., Faraday Trans. 2* **1974**, *70*, 2004, and references therein.

(16) (a) Eland, J. H. D. *Photoelectron Spectroscopy: An Introduction to Ultraviolet Photoelectron Spectroscopy in the Gas Phase*; Butterworth: London, 1974. (b) Kimura, K.; Katsumata, S.; Achiba, Y.; Yamazaki, T.; Iwata, S. *Handbook of He I Photoelectron Spectra of Fundamental Organic Molecules*; Japan Scientific Societies Press: Tokyo, 1981.

(17) (a) Lloyd, D. R.; Lynaugh, N. *Philos. Trans, R. Soc. London, A* **1970**, *268*, 97. (b) Brundle, C. R.; Robin, M. B.; Basch, H.; Pinsky, M.; Bond, A. *J. Am. Chem. Soc.* **1970**, *92*, 3863. (c) Rose, T.; Frey, R.; Brehm, B. *J. Chem. Soc., Dalton Trans.* **1969**, 1518. (d) Asbrink, L.; Svensson, A.; Von Niessen, W.; Bieri, G. *J. Electron Spectrosc. Relat. Phenom.* **1981**, *24*, 293. (e) Dyke, J. M.; Haggerston, D.; Warschkow, O.; Andrews, L.; Downs, A. J.; Souter, P. F. *J. Phys. Chem.* **1996**, *100*, 2998.

(18) Lloyd, D. R.; Lynaugh, N.; Robberts, P.; Guest, M. F. *J. Chem Soc. Faraday Trans. 2* **1975**, *71*, 1382.

(19) Ulman, J. A.; Fehlner, T. P. *J. Am. Chem. Soc.* **1978**, *100*, 449, and references therein.

(20) (a) Lipscomb, W. N. *Pure Appl. Chem.* **1983**, *55*, 1431. (b) Page, M.; Adams, G. F.; Binkley, J. S.; Melius, C. F. *J. Phys. Chem.* **1987**, *91*, 2675. (c) Horn, H.; Ahlrichs, R.; Kölmel, C. *Chem. Phys. Lett.* **1988**, *150*, 263.

(21) Hehre, W. J.; Radom, L.; Schleyer, P. v. R.; Pople, J. A. *Ab initio Molecular Orbital Theory*; Wiley−Interscience: New York, 1986.

(22) Stanton, J. F.; Lipscomb, W. N.; Bartlett, R. J.; McKee, M. L. *Inorg. Chem.* **1989**, *28*, 109.

(23) (a) Cederbaum, L. S.; Domcke, W. *Adv. Chem. Phys.* **1977**, *26*, 1023. (b) Öhrn, Y.; Born, G. *Adv. Quantum Chem.* **1981**, *13*, 1.

(24) (a) Ortiz, J. V. *J. Chem. Phys.* **1996**, *104*, 7599. (b) Ferreira, A. M.; Seabra, G.; Dolgounitcheva, O.; Zakrzewski, V. G.; Ortiz, J. V. In *Quantum−Mechanical Prediction of Thermochemical Data*; Cioslowski, J., Ed.; Kluwer: Dordrecht, The Netherlands, 2001; p 131. (c) Seabra, G.; Zakrzewski, V. G.; Ortiz, J. V. In *Structures and Mechanisms From Ashes to Enzymes*; Eaton, G. R., Wiley, D. C., Jardetzky, O., Eds.; ACS Symposium Series, Vol. 827; American Chemical Society: Washington, DC, 2002; p 118. (Distributed by Oxford University Press.)

(25) (a) Ramakrishna, V.; Duke, B. J. *Inorg. Chem.* **2004**, *43*, 8176. (b) Hollins, R. E.; Stafford, F. E. *Inorg. Chem.* **1970**, *9*, 877.

(26) Frisch, M. J.; Trucks, G. W.; Schlegel, H. B.; Scuseria, G. E.; Robb, M. A.; Cheeseman, J. R.; Zakrzewski, V. G.; Montgomery, J. A., Jr.; Stratmann, R. E.; Burant, J. C.; Dapprich, S.; Millam, J. M.; Daniels, A. D.; Kudin, K. N.; Strain, M. C.; Farkas, O.; Tomasi, J.; Barone, V.; Cossi, M.; Cammi, R.; Mennucci, B.; Pomelli, C.; Adamo, C.; Clifford, S.; Ochterski, J.; Petersson, G. A.; Ayala, P. Y.; Cui, Q.; Morokuma, K.; Malick, D. K.; Rabuck, A. D.; Raghavachari, K.; Foresman, J. B.; Cioslowski, J.; Ortiz, J. V.; Baboul, A. G.; Stefanov, B. B.; Liu, G.; Liashenko, A.; Piskorz, P.; Komaromi, I.; Gomperts, R.; Martin, R. L.; Fox, D. J.; Keith, T.; Al-Laham, M. A.; Peng, C. Y.; Nanayakkara, A.; Gonzalez, C.; Challacombe, M.; Gill, P. M. W.; Johnson, B.; Chen, W.; Wong, M. W.; Andres, J. L.; Gonzalez, C.; Head-Gordon, M.; Replogle, E. S.; Pople, J. A. *GAUSSIAN 98*; Gaussian, Inc.: Pittsburgh, PA, 1998.

(27) (a) Møller, C.; Plesset, M. S. *Phys. Rev.* **1934**, *46*, 618. (b) Frisch, M. J.; Head-Gordon, M.; Pople, J. A. *Chem. Phys. Lett.* **1990**, *166*, 281.

(28) (a) Bartlett, R. J. *J. Phys. Chem.* **1989**, *93*, 1697. (b) Kucharski, S. A.; Bartlett, R. J. *Adv. Quantum Chem.* **1986**, *18*, 281. (c) Bartlett, R. J.; Stanton, J. F. In *Reviews of Computational Chemistry*; Lipkowitz, K. B., Boyd, D. B., Eds.; VCH Publishers: New York, 1995; Vol. V, Chapter 2, p 65.

(29) Schaftenaar, V. *MOLDEN*; CAOS/CAMM Center: The Netherlands, 1991.

(30) Kawaguchi, K. *J. Chem. Phys.* **1992**, *96*, 3411.

(31) Callomon, J. H.; Hirota, E.; Kuchitsu, K.; Lafferty, W. J.; Maki, A. G.; Pote, C. S. *Structural Data on Free Polyatomic Molecules*; Springer: Berlin, 1976; Vol. 7.

(32) Weaver, J. R.; Hertsch, C. W.; Parry, R. W. *J. Chem. Phys.* **1959**, *30*, 1075.

(33) Hrostowski, H. J.; Meyers, R. J.; Pimentel, G. C. *J. Chem. Phys.* **1952**, *20*, 518.

(34) Guerra, C. F.; Bickelhaupt, F. M.; Snijders, J. G.; Baerends, E. *J. Am. Chem. Soc.* **2000**, *122*, 4117.

(35) Kaldor, A.; Porter, R. F. *J. Am. Chem. Soc.* **1971**, *46*, 1444.

(36) (a) Kawaguchi, K.; Butler, J. E.; Bauer, S. H.; Minowa, T.; Kanamori, H.; Hirota, E. *J. Chem. Phys.* **1992**, *96*, 3411. (b) Jacox, M. E. *J. Phys. Chem. Ref. Data* **1994**, (Monograph 3), 124−126.

(37) Shimanouchi, T. *Tables of Molecular Vibration Frequencies Consolidated*; NSRDS−NBS 39; NBS, U.S. Government Printing Office: Washington, DC, 1972; Vol. 1.

(38) NIST Chemistry WebBook, http://webbook.nist.gov/chemistry (IR spectrum of *ara*-B_4H_{10}).

(39) Chase, M. W., Jr.; Davies, C. A.; Downey, J. R., Jr.; Frurip, D. J.; MacDonald, R. A.; Syverud, A. N. *J. Phys. Chem. Ref. Data* **1985**, *14*, Suppl. 1.

(40) Berkowitz, J.; Greene, J. P.; Cho, H.; Ruščić, B. *J. Chem. Phys.* **1987**, *86*, 674.

(41) Cederbaum, L. S. *J. Phys. B* **1975**, *8*, 290.

(42) (a) Blum, E.; Herzberg, G. *J. Phys. Chem.* **1937**, *41*, 91. (b) Price, W. C. *J. Chem. Phys.* **1947**, *15*, 614. (c) Price, W. C. *J. Chem. Phys.* **1948**, *16*, 894. (d) The conventional assignments were used in these studies.

(43) (a) Schirmer, J.; Cederbaum, L. S.; Walter, O. *Phys. Rev. A* **1983,** *28*, 1237. (b) von Niessen, W.; Schirmer, J.; Cederbaum, L. S. *Comput. Phys. Rep.* **1984**, *1*, 57. (c) Schirmer, J.; Angonoa, G. *J. Chem. Phys.* **1989**, *91*, 1754.

(44) Nakatsuji, H. In *Computational Chemistry−Reviews of Current Trends*; Leszczynski, J., Ed.; World Scientific: Singapore, 1997; Vol. 2.

(45) For example: (a) Tian, S. X.; Chen, X. J.; Xu, C. K.; Xu, K. Z.; Yuan, L. F.; Yang, J. L. *J. Electron Spectrosc. Relat. Phenom.* **1999**, *105*, 99, and references therein. (b) Tian, S. X.; Kishimoto, N.; Ohno, K. *J. Phys. Chem. A* **2002**, *106*, 6541, 7714; **2003**, *107*, 53, 485, 2137. (c) For a recent review, see: Ohno, K.; Yamazaki, M.; Meada, S.; Kishimoto, N. *J. Electron Spectrosc. Relat. Phenom.* **2005**, *142*, 283.

(46) Paine, R. T.; Sodeck, G.; Stafford, F. E. *Inorg. Chem.* **1972**, *11*, 2593.

(47) Fehlner, T. P. *Inorg. Chem.* **1975**, *14*, 934.

(48) Johes, R. W.; Koski, W. S. *J. Chem. Phys.* **1973**, *59*, 1228.